Journal of Applied Fluid Mechanics, Vol. 16, No. 9, pp. 1839-1852, 2023.
Available online at www.jafmonline.net, ISSN 1735-3572, EISSN 1735-3645.
https://doi.org/10.47176/jafm.16.09.1808

A Novel Vane-twisted Conformal Diffuser for Compact Centrifugal Compressors

X. X. Yang and Y. Liu†

School of Energy and Power Engineering, Dalian University of Technology, No. 2 Linggong Road, Ganjingzi District, Dalian 116024, China

†*Corresponding Author Email†: yanliu@dlut.edu.cn*

ABSTRACT

Compact aero-engines that use centrifugal compressors are in high demand due to their small size and cost-effectiveness. However, limited improvements in the aerodynamic performance of centrifugal impellers have led to a greater focus on improving the performance of diffusers. This paper introduces a novel vane conformal diffuser designed to match an impeller with a high pressure ratio. The diffuser utilizes a unique design method that creates transitions from a two-dimensional meridian to a three-dimensional configuration, to achieve a twisted design for the vane and hub. Eventually an integrated vane configuration is formed from the radial section to the bend and axial sections. The novel diffuser significantly reduces the radial size of the entire compressor compared with a conventional vaned diffuser. Different cross-section area distributions are studied to explore the reasonable static pressure recovery ability of the diffuser. To validate the new concept, the diffusers of two existing high-pressure centrifugal compressors are redesigned using the novel conformal diffuser configuration. The numerical results show that the aerodynamic performances of the two redesigned centrifugal compressors are improved in terms of both the total pressure ratio and the isentropic efficiency compared with their counterparts. These results demonstrate the effectiveness and applicability of the developed design method for the novel conformal diffuser.

Article History

Received February 9, 2023
Revised April 11, 2023
Accepted April 28, 2023
Available online July 1, 2023

Keywords:

Vaned-twisted
Conformal diffuser
Compact centrifugal compressor
Numerical simulation
Turbomachinery

1. INTRODUCTION

With the thrust-to-weight ratio continually increasing, compact centrifugal compressors have become increasingly attractive and are now widely used in small aero-engines due to their small size and light weight. Increasing the pressure ratio of a compact centrifugal compressor helps to improve the performance of aero-engines. However, this increase in the pressure ratio also results in a higher Mach number and smaller tangential flow angles at the impeller outlet, both of which present challenges to the design of the downstream component, i.e., the diffuser, particularly when the available radial space is limited. Therefore, researchers have been pursuing the design of an efficient diffuser that offers reasonable diffusion and minimal total pressure loss for high pressure ratio centrifugal compressors.

Vaned diffusers have been commonly used in high pressure ratio centrifugal compressors, where segmented diffusers have been traditionally employed. These diffusers typically consist of a radial vaned diffuser, a vaneless turning section, and an axial vaned diffuser for gas turbine applications. In 1982, Rodgers (Rodgers, 1982) introduced six common segmented diffusers including Profiled, Channel (Wedged), Slotted, Pipe, Splitter and Tandem diffusers. To investigate the impact of the inlet geometrical parameters of a radial vaned diffuser, the author conducted experimental research on the commonly used channel diffuser. The results showed that the radial vaned diffuser could be adapted to high Mach number flows as long as the throat area of the vaned diffuser was reasonable. In another study, Krige (Krige, 2013) investigated the radial section area of a segmented diffuser for a centrifugal compressor with a pressure ratio of 2.7 applied to a micro gas turbine BMT 120KS. The author obtained a radial vaned diffuser with better performance by adjusting the shapes of the original wedged diffuser three times. De Villiers (De Villiers, 2014) designed and optimized an airfoil shaped radial vaned diffuser for a centrifugal impeller with a total pressure ratio of four, used in a Micro Gas Turbine. The

Nomenclature

C_p	static pressure recovery coefficient	β_A	blade tangential angle
C_{pt}	total pressure loss coefficient	φ	flow coefficient
D	diameter	**Subscript**	
l	axial length	1	impeller inlet
n	rotational speed	2	impeller outlet
P	static pressure	3	radial diffuser inlet
P^*	total pressure	4	hub of axial diffuser
Z	blade number	5	shroud of axial diffuser

camber line of the diffuser vane was defined by a logarithmic function, and the results showed that this design method easily optimized vaned diffusers with high performance. Wang et al. (Wang et al., 2018) studied a radial wedged vaned diffuser of a centrifugal compressor with a total pressure ratio of four and found that more vanes resulted in a lower inlet Mach number and reduced separation in the wedge passage, leading to improved efficiency. Hayami (Hayami, 2000) designed a low solidity radial vaned diffuser with double circular arc vanes. By reducing the width of the impeller blades at the outlet of the impeller and the inlet passage width of the diffuser for a compressor with a pressure ratio of six, the input power was reduced, and the efficiency was significantly improved. Jiang (Jiang, 2016) designed a segmented diffuser for an impeller with a total pressure ratio of 11.7 and conducted further studies on the radial wedged diffuser, demonstrating that the efficiency of the wedged diffuser with an inlet contraction was 2.7% higher than that of a wedged diffuser without an inlet contraction.

The studies mentioned above indicate that improved performance for radial vaned diffusers can be achieved by optimizing key geometric parameters and modifying their shape, as evidenced by various references (Oh & Agrawal, 2007; Oh, Buckley and Agrawal 2008; Oh, Buckley and Agrawal 2012; Xiang et al., 2018). However, the use of radial vaned diffusers in limited radial spaces poses a challenge due to limited diffusion, particularly for high Mach inlet flows (Han et al. 2018). In addition, segmented diffusers have not been able to fully address the issue of separation (Benini & Toffolo, 2003; Chen, 2010; Burger, 2016). Therefore, new types of diffusers, such as conformal diffusers developed from conventional pipe diffusers, have been developed to meet the compactness constraint for aero-engines in recent years.

The radial passages of a conventional pipe diffuser consist of a series of drillings arranged symmetrically in a radial plane, with their center lines tangent to the same circle. This type of diffuser performs well for inlet supersonic Mach numbers and asymmetrical flow (Kenny, 1969; Zachau et al., 2009). In addition, fishtail pipe diffusers are used in the bend and axial passages to turn the flow from the radial direction to the axial direction, improving the efficiency of the centrifugal compressor stage (Kenny, 1969; Han et al., 2018). Conventional pipe diffusers are not only compact and cost-effective, but also easy to manufacture, making them suitable for various small aero-engines (Kenny, 1969; Wrong, 1981; Moustapha, 2003; Bourgeois et al., 2009). However, each fishtail pipe diffuser is processed separately, inserted into the radial pipe diffuser one by one, and attached with bolts to connect to the diffuser base, resulting in a large number of parts (Kenny, 1969; Han et al., 2017). With the development of advanced manufacturing technologies, radial and fishtail sections can be integrated to form a whole configuration, eliminating the need for segmentation. (Moustapha, 2003). This novel pipe diffuser is also known as a conformal diffuser (Chen, 2010). However, limited literature has been published on these types of conformal diffusers due to confidential reasons.

Robert et al. (Roberts et al., 2003) tested a conformal diffuser on a GR180 turbojet engine for small UAVs and found that it performed better than a segmented diffuser. Czarnecki and Olsen (Czarnecki & Olsen, 2018) developed a simplified design method for a conformal diffuser by summarizing the geometric and aerodynamic parameters of GT60, TK50, MW54, and KJ66 turbojet engines. Burger (Burger, 2016) added a three-element vane to a conformal diffuser structure and showed that it outperformed a conventional segmented diffuser. Chen et al. (Chen & Huang, 2010, Chen, Yue and Huang 2014) designed and studied a conformal diffuser for a small turbojet engine with splitter vanes, and found that a convex form was the optimal cross-sectional area distribution for the passage. They also explored the flow mechanism of the diffuser. By summarizing the existing design methods and performance characteristics of the conformal diffuser, it was found that the configuration of the conformal diffuser was essentially an extension of the radial vane of the diffuser to the bend section and the axial diffuser. However, designs that abandon a fishtail structure, such as a conventional pipe diffuser, can lead to separation in the bend and axial passages due to the sudden expansion in the cross-section area. To address this, Burger (Burger, 2016) increased the curvature radius of the bend section, but this also increased the axial length of the diffuser, making it longer than the segmented diffusers. Chen et al. (Chen & Huang, 2010; Chen et al., 2014) solved this issue by increasing the thicknesses of the bend and axial blades and adding splitters in the downstream section of each main passage. However, these methods were difficult to design and manufacture and greatly increased the weight of the diffuser.

In this paper, we propose a novel conformal diffuser that differs from the previously mentioned integrated conformal diffuser (see Fig. 1(a)). The radial vane is twisted directly into a part of one axial vane, and the radial hub is changed directly to one surface of the axial

(a) Conventional conformal diffuser (Krige, 2013)

(b) New conformal diffuser

(c) Segmented diffuser (Burger, 2016)

Fig. 1. Three types of diffusers for centrifugal compressors used in aero-engines.

vane, as shown in Fig. 1 (b). This innovative configuration has proven to be very efficient within a limited radial and axial dimension and can be easily adjusted for the cross-section area to further enhance the diffuser performance. A conventional radial and axial diffuser (or segmented diffuser) is also presented in Fig. 1 (c) for comparison.

2. CONFIGURATION DESCRIPTION OF THE NOVEL CONFORMAL DIFFUSER

Figure 2 illustrates the meridional channel of a centrifugal compressor featuring the proposed novel conformal diffuser. D_2 is the impeller outlet diameter. D_3 is the diffuser inlet diameter. D_4 and D_5 are the hub and shroud diameters at the axial outlet respectively. Prior to

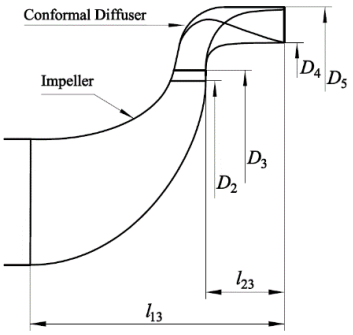

(a) Meridional channel

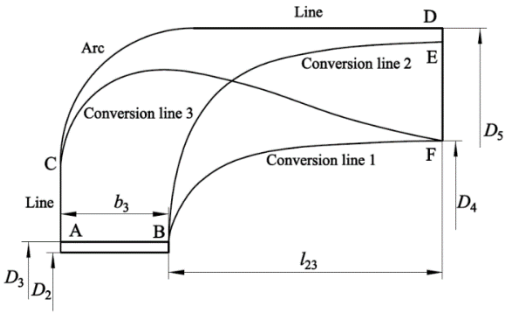

(b) Zoom in diffuser part

Fig. 2. Meridional channel of a centrifugal compressor with a novel conformal diffuser.

designing a diffuser to match the impeller, fluid flow parameters such as the flow angle, Mach number, and pressure at the outlet of the impeller i.e. the inlet of the diffuser should be known. Moreover, the maximum D_5 and the maximum axial distance l_{23} must be specified.

2.1 Meridional Design

The profiles of the vane tip, root, leading edge, and trailing edge of both segmented and conventional conformal diffusers can be adjusted by reducing their dimensions in the meridional channel. As shown in Fig. 2, the new conformal diffuser proposed in this paper differs from both segmented and conventional conformal diffusers in that its twisted vanes cannot be projected onto a regular meridional channel, resulting in the absence of a regular hub, vane tip, and root that rotate along the axis. However, by introducing three conversion lines, a plane geometry similar to the meridional channel can be obtained, allowing for convenient adjustment of geometric parameters, such as the cross-section area.

In Fig. 2, line AB represents the leading edge of the diffuser vane, and line DF represents the trailing edge. To match the adjacent outer casings, the shroud curve AD adopts the form of a straight line (wedged vane) and an arc (the intermediate part between the wedged vane and the axial vane) and a straight line (axial vane) on the pressure side. The curve BF serves as conversion line 1 and is not the projection of the hub; instead, it connects the hub of the wedged vane on the pressure side and the root of the adjacent axial vane on the suction side. The curve can be composed of a Bezier curve or a Spline curve. Conversion line 2 consists of the hub on the suction side of the wedged vane and the shroud of the axial vane, making a 90-degree bend that transitions smoothly. Conversion line 3 starts from the turning point

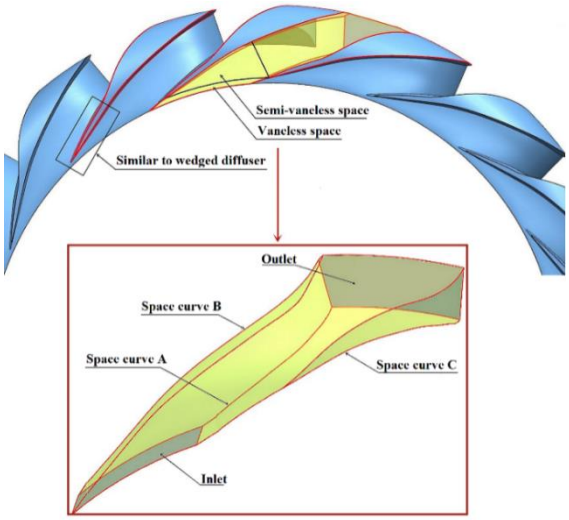

(a) Structure of a single passage

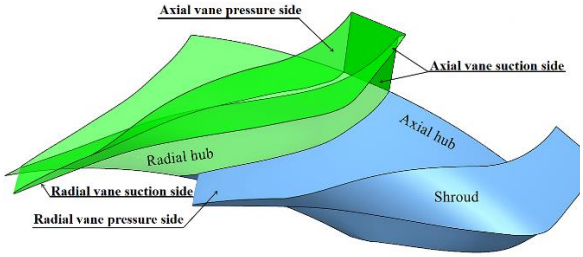

(b) Structure of a vane

Fig. 3. Configuration of the novel conformal diffuser.

C of the wedged vane tip on the shroud to the shroud of the axial vane trailing edge on the pressure side. Conversion lines 2 and 3 can also be composed of a Bezier or a Spline curve. Lines can be used to form the surfaces of diffuser vanes and one flow passage.

With the above mentioned design, the positions of points A, B, D, E, and F are established. Therefore, by adjusting the positions of the control points of conversion lines 1, 2, and 3, the relevant geometric parameters of the diffuser passages can be modified.

2.2 Three-Dimensional Configuration

To effectively design the diffuser flow passage in a small space with a large turning angle, the novel conformal diffuser not only integrates the radial, bend, and axial sections but also twists each vane in space. Therefore, it is necessary to flexibly control the geometrical parameters of different sections of the flow passage to ensure a reasonable diffusion ratio and avoid flow separation.

Figure 3 depicts the structure of the novel conformal diffuser. As shown in Fig. 3 (a), the radial section consists of wedged vanes because they are suitable for high Mach number inflows. At the end of a wedged vane, the vane begins to be twisted and coupled with the radial hub as mentioned before. This can be seen in Fig. 3 (b), where the suction side of a wedged vane and the hub are twisted downstream to form the suction side of an axial diffuser vane through space curves A and B. Part of the pressure side of the wedged vane continues to stretch and form the pressure side of the axial vane through the space curve C, while the other part is gradually twisted into the hub of the axial vane. During the twist of the diffuser vanes, the shroud remains unchanged. Using the above mentioned twist methods, the structure of a single flow passage of a novel conformal diffuser can be obtained.

During the entire twisting process, space curves A and B can be adjusted using conversion lines 1 and 2 based on the given inlet and outlet vane angles. Similarly, space curve C can be adjusted using conversion line 3. The introduction of space curve C changes the cross-section shape of the novel conformal diffuser from an irregular quadrilateral in the radial section to an irregular pentagon in the bend and axial sections.

The design of a twisted vane in the novel conformal diffuser ensures a relatively smooth flow passage and improves flow stability. This configuration is suitable for applications with limited space and can reduce the degree of diffuser vane twist while still achieving the necessary change in flow direction from radial to axial within a small radial space. Moreover, the twisting process allows for flexible adjustment of the cross-section area without altering the size or blade thickness, ensuring a reasonable diffusion ratio for the bend and axial sections. Overall, the novel conformal diffuser combines the advantages of conventional conformal diffusers with the benefits of vane twist design, making it a highly adaptable and efficient solution for diffuser design in small aero-engine applications.

3. VERIFICATION OF NUMERICAL METHOD

In this research, ANSYS CFX 17.0 is used to conduct numerical simulations. The 3D RANS equations and the energy equation for an ideal gas (air) are solved using a coupled implicit pressure-based solution technique. A “High Resolution” advection scheme, which is a second-order scheme and bounded, is used to discretize advection and diffusion fluxes in the governing equations. The SST turbulence model with automatic wall functions is used to calculate Reynolds stresses.

To validate the accuracy of the numerical method used in this research, a centrifugal compressor named HECC (Medic et al., 2014) is selected as a validation case. The 3D geometry of the HECC is shown in Fig. 4 (a). The HECC is used in an aero-engine and consists of an impeller, a vaned diffuser with splitter vanes, and an exit guide vane, as shown in Fig. 4 (a). The design speed and total pressure ratio of the HECC are 21789 rpm and 4.5, respectively. To save computing time, a single passage of the HECC is used for the computational domain. According to reference (Li et al., 2021), a grid independence study is carried out, and a structured grid with 6293628 nodes is generated. At the inlet of the HECC, total pressure and total temperature are given as boundary conditions, and the mass flow is specified at the outlet. All solid walls in the computational domain are assumed to be adiabatic, smooth, and no-slip.

In Fig. 4(b), the predicted total pressure ratio and isentropic efficiency from CFX and experimental data for the HECC are compared. It can be observed that the

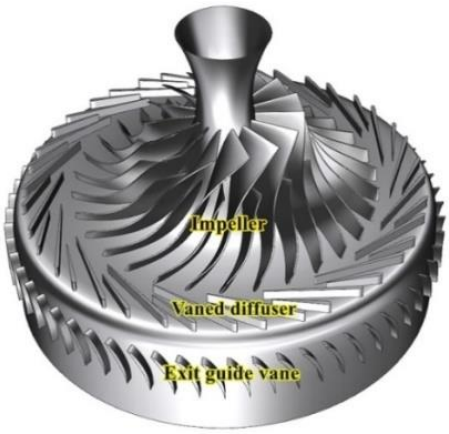

(a) HECC geometry

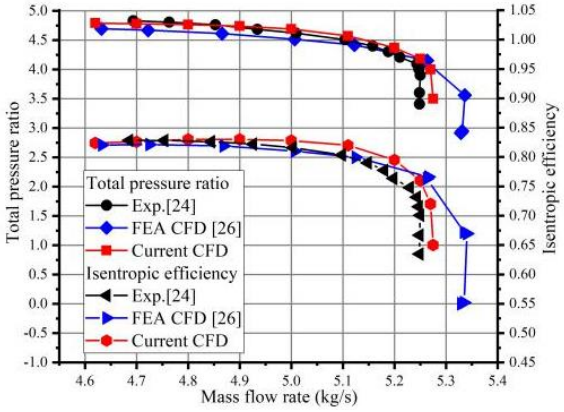

(b) Comparison of experimental results and CFD

Fig. 4. 3D HECC geometry and CFD results.

numerical predictions agree well with the measurements. The figure also presents the results from reference (TCAE-CFD) for comparison, which further confirms the accuracy of the current numerical method. The choking phenomenon greatly reduces the total pressure ratio and isentropic efficiency at the large flow rate. This result validates the reliability and accuracy of the current numerical method and its applicability to other cases investigated in this research.

4. ANALYSIS OF CROSS-SECTION AREA DISTRIBUTION

A compact centrifugal compressor with a total pressure ratio of four was designed with a novel conformal diffuser using the developed design method. The 3D geometry of the compressor is presented in Fig. 1 (b), and some key parameters are given in Table 1.

Because the distribution of the cross-sectional area is considered the most important parameter affecting the performance of a vaned diffuser (Chen & Huang, 2010), it is crucial to explore the optimal distribution of the cross-sectional area to obtain a conformal diffuser with superior performance. The cross-section area distribution referred to here is the variation of the cross-section area from the throat to the outlet of a single passage, as illustrated in Fig. 5.

Table 1 Key parameters of the compressor

Parameter	Variable	Value
Relative position of shroud	D_5/D_2	1.28
Relative position of hub	D_4/D_2	1.15
Relative position of diffuser inlet	D_3/D_2	1.01
Axial length ratio	l_{23}/l_{13}	0.33
Number of impeller blades	Z_{imp}	7+7
Number of diffuser blades	Z_{dif}	17
Total pressure ratio of impeller (at design)	ε_2	4.6
Outlet Mach number of impeller (at design)	Ma_2	0.98

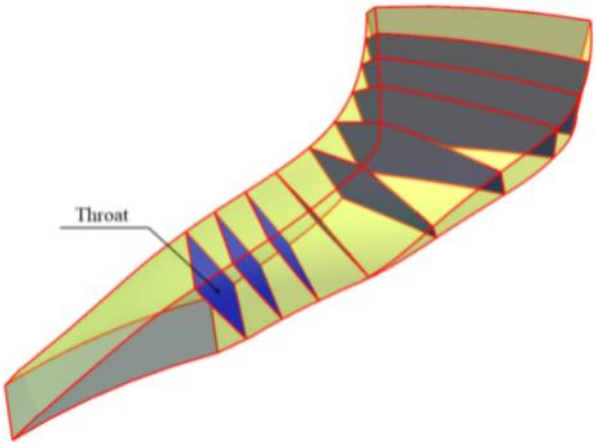

Fig. 5. Cross-sections of a single passage.

Four different distributions of the cross-sectional area are shown in Fig.6. Scheme 1 shows a convex variation, Scheme 2 shows a concave variation, and Scheme 3 shows a linear variation. Schemes 2 and 3 have abrupt variations at their outlets and inlets, respectively, leading to an excessive local diffusion ratio, an adverse pressure gradient, and flow separation, leading to greater losses. Scheme 4 has a smooth transition between the inlet part of Scheme 2 and the outlet part of Scheme 3. While designing Scheme 1, interference between adjacent passages arises due to the large cross-section area in the middle of the passage. To avoid interference, the curvature radius of Scheme 1 is increased, making it similar to Scheme 3. Therefore, Scheme 1 is not considered further.

To perform numerical simulations on the designed centrifugal compressor, a single passage computational domain is used, as shown in Fig. 7(a). A structured grid is generated using NUMECA Autogrid V5 for the impeller and inlet domains, while the diffuser and outlet extended domain are meshed with a structured grid generated using ICEM. The grid is shown in Fig. 7(b). High precision and meticulous care are applied to preserve the boundary layer by adjusting the first-layer grid height close to the solid walls to ensure there is enough resolution near the solid walls and blade/vaned boundary layers. Therefore, as shown in Fig. 7(c), the value of y plus is less than 2. The numerical schemes applied are the same as before.

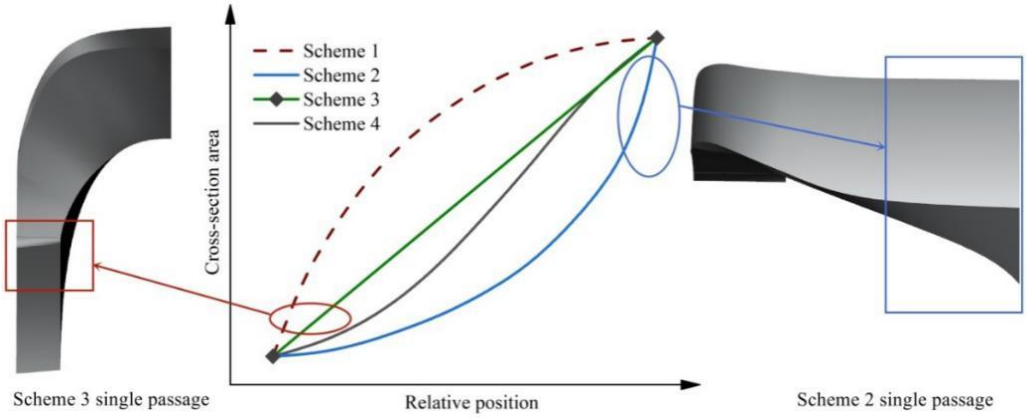

Fig. 6. Different distributions of cross-section area.

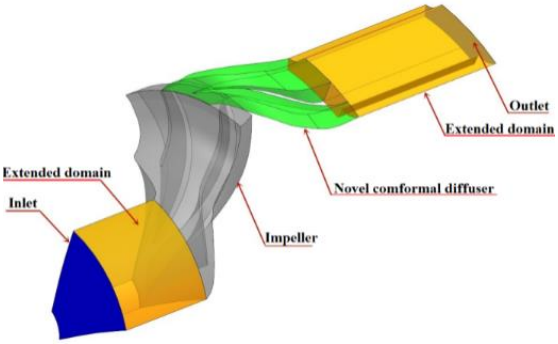

(a) All computation domains

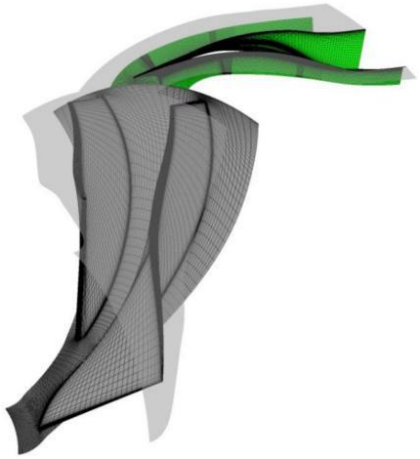

(b) Impeller and diffuser grids

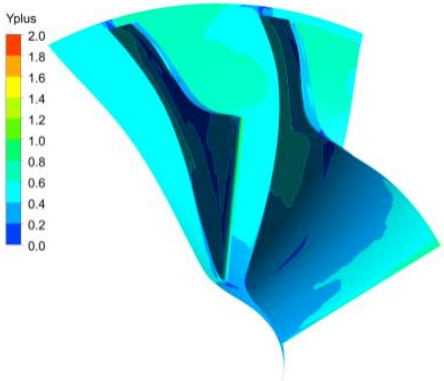

(c) y plus

Fig. 7. Schematic diagram of the computational domain and computational grid.

Table 2. Study of grid independence

Component	Grid level	ε_2	Difference
Impeller	Coarse	4.5043	1.368%
	Medium 1	4.5329	0.744%
	Medium 2	4.5563	0.231%
	Fine	4.5668	-
	Grid level	C_p	Difference
Scheme 4	Coarse	0.61395	1.644%
	Medium 1	0.61918	0.806%
	Medium 2	0.62247	0.279%
	Fine	0.62421	-

The grid independence of the solutions is studied using different sets of mesh sizes. For Scheme 4, the total pressure ratio (ε_2) for the impeller and the static pressure recovery coefficient (C_p) for the diffuser are evaluated for different grids. As shown in Table 2, the difference between the Medium 2 grid and the fine grid is less than 0.28% for both the impeller and diffuser. A similar result is also observed for Schemes 2 and 3. Therefore, the Medium 2 grid is selected for the remaining simulations.

Figure 8 shows predicted performance results for the compressor with different schemes. It can be observed from Fig. 8 that the total pressure ratio for Scheme 2 is higher than that of Scheme 3, with a maximum difference of 1.5%. The relative isentropic efficiencies for the three schemes are all divided by the efficiency of Scheme 4 at the design point to obtain relative values. The relative isentropic efficiency of Scheme 3 is slightly higher than that of Scheme 2 except for large flow coefficient conditions. The reason for the curve crossing is that the flow separation is slightly severe at the inlet for large flow conditions in Scheme 3 (see Fig.11). Compared with Schemes 2 and 3, the aerodynamic performance of Scheme 4 is improved for the whole operating range. Furthermore, the highest efficiency point of Scheme 4 is at the design point while Schemes 2 and 3 have deviations.

The other two important parameters used to evaluate diffuser performance are the static pressure recovery coefficient (C_p) and the total pressure loss coefficient (C_{pt}). C_p refers to the percentage of the inlet dynamic

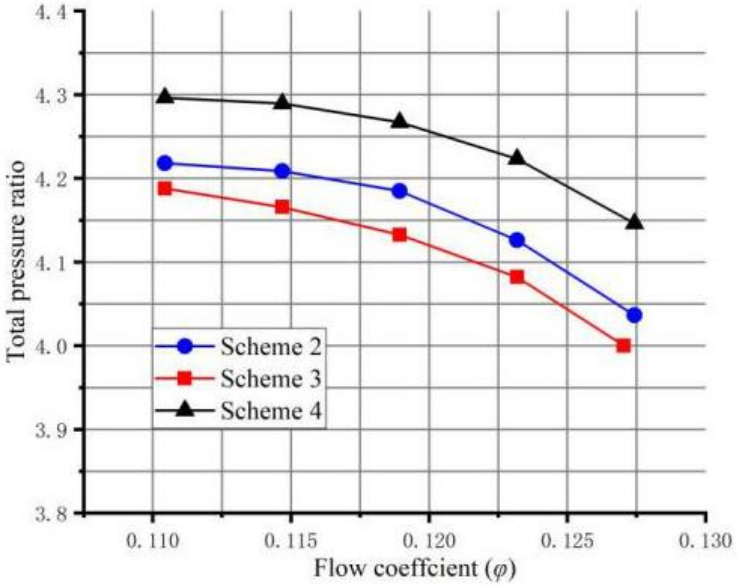

(a) Total pressure ratio

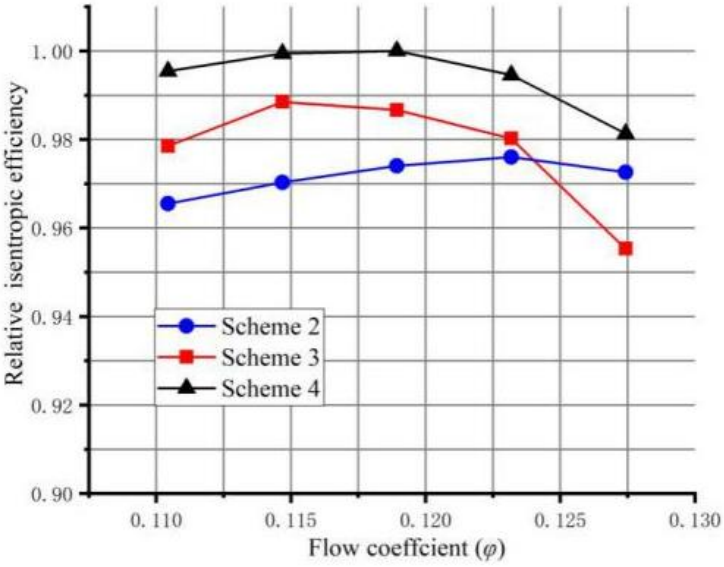

(b) Relative isentropic efficiency

Fig. 8. Performance comparison for the compressor with different schemes.

pressure that is converted to static pressure through the diffuser, and C_{pt} refers to the percentage of total pressure loss through the diffuser to inlet dynamic pressure. The formulas for C_p and C_{pt} are given in Equations (1) and (2), respectively:

$$C_p = (P_4\text{-}P_3)/\left(P_3^*\text{-}P_3\right) \tag{1}$$

$$C_{pt} = (P_3^*\text{-}P_4^*)/\left(P_3^*\text{-}P_3\right) \tag{2}$$

where P_3* and P_3 are the total pressure and static pressure at the inlet of the diffuser, respectively, and P_4* and P_4 are the total pressure and static pressure at the diffuser outlet, respectively. The CFD-predicted C_p and C_{pt} are shown in Fig.9 for the three schemes. The C_p and C_{pt} curves of Schemes 2 and 3 cross, for the same reason as that of the efficiency curves. In addition, similar to the total pressure ratio and isentropic efficiency, Scheme 4 performs the best and gives the best results for the whole working range.

Entropy generation Δs is another crucial parameter used to evaluate the loss in the diffuser. Fig.10 shows the normalized static entropy generation from the inlet to the outlet of the diffuser for the three schemes at different flow conditions. Because the essence of total pressure loss is entropy generation, the trend of entropy generation is consistent with Fig. 9 (b). Formula (3) is the calculation method for entropy generation from the inlet to the outlet of the diffuser.

$$\Delta s = \left(\ln P_3^* - \ln P_4^*\right)/R \tag{3}$$

Formula (4) is obtained by applying Formula (3) to Formula (2):

$$C_{pt} = \frac{P_3^*}{P_3^*\text{-}P_3}\left(1\text{-}e^{-\frac{\Delta s}{R}}\right) \tag{4}$$

where R is the gas constant. Because P_3^* and P_3 are impeller outlet parameters, it can be explained that the trend of C_{pt} is consistent with that of Δs through the

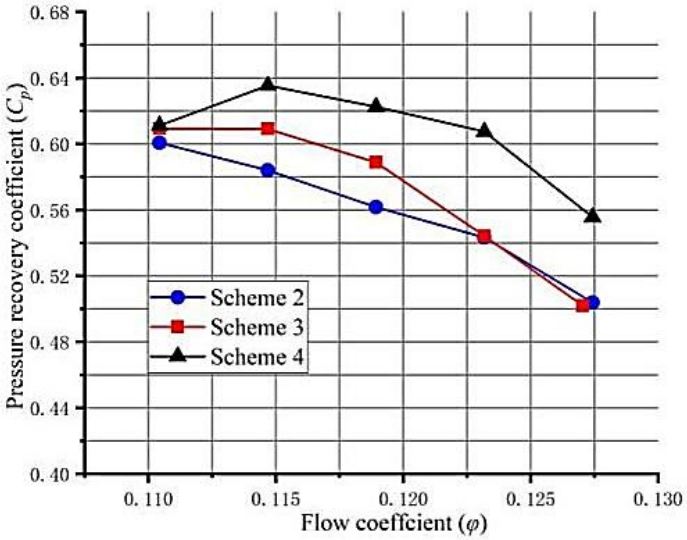

(a) Pressure recovery coefficient

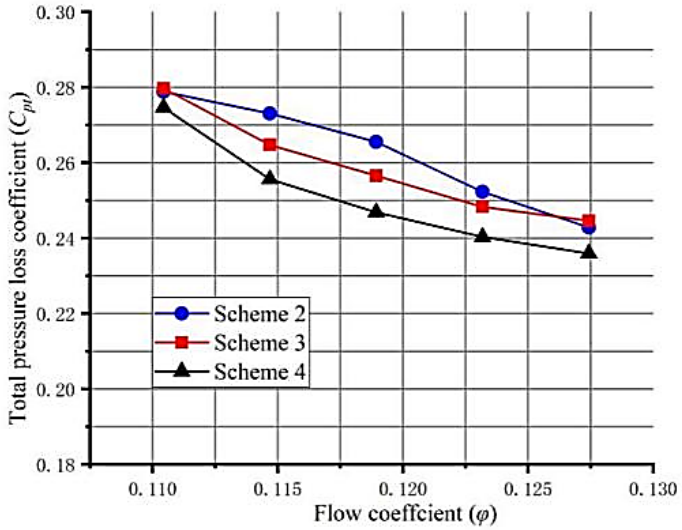

(b)Total pressure loss coefficient

Fig. 9. Comparison of static pressure recovery and total pressure loss coefficients

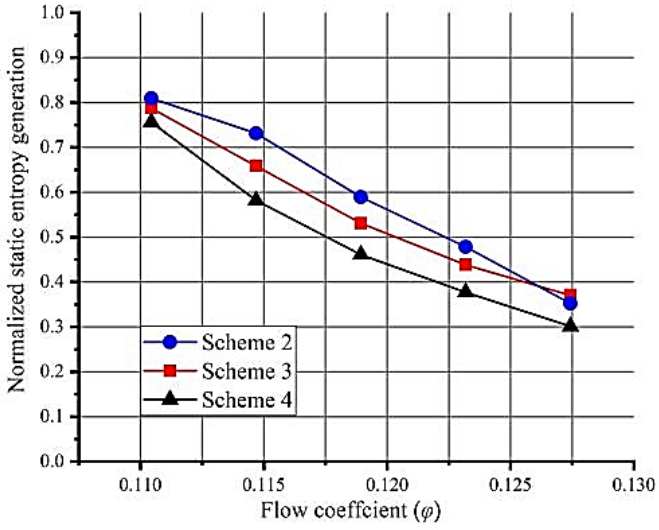

Fig. 10. Comparison of normalized static entropy generation

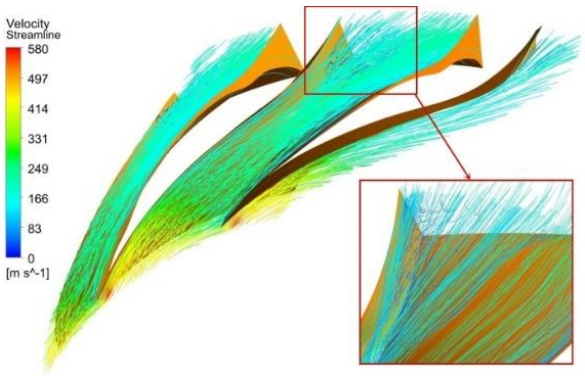

(a) Scheme 2

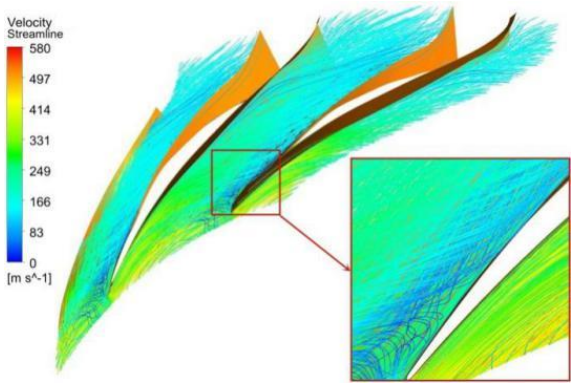

(b) Scheme 3

(c) Scheme 4

Fig. 11. 3D streamline comparisons for the three schemes at the design point.

property of the exponential function. Therefore, the total pressure loss coefficient can express the entropy generation.

Figure 11 shows the 3D streamline distributions for the three schemes at the design point. Due to the strong 3D nature of the new conformal diffuser, it is challenging to depict the streamlines on 2D planes. As observed from the figure, there is obvious flow separation near the suction side of the diffuser vane at the outlet for Scheme 2 and on the pressure side of the diffuser vane at the inlet for Scheme 3. However, for Scheme 4, there is no obvious flow separation and the flow is stable. The flow field demonstrates the superiority of Scheme 4.

It can be deduced that a conformal diffuser configuration must have a reasonable cross-section area distribution and a diffusion factor similar to Scheme 4 to match its corresponding impeller. Applications of the design theory described above to two other high-pressure centrifugal compressors are given in the next section.

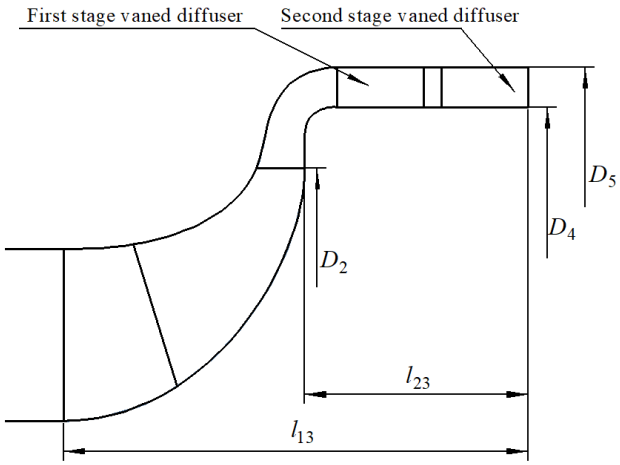

Fig. 12. Meridional channel of the original model of case A.

5. VERIFICATION OF THE DEVELOPED DESIGN THEORY

5.1 Case A

Case A is a self-designed centrifugal compressor for an aero-engine with a total pressure ratio of five. As it is required that D_5/D_2 should be very small, at 1.33 in the design specifications, there is not enough radial space to place a radial vaned diffuser.

The original design scheme only adopts an axial tandem diffuser, as can be seen in the meridional channel shown in Fig. 12. However, numerical simulations (see Fig. 13) reveal that the total pressure ratio and isentropic efficiency at the design point (corresponding to a flow coefficient of 0.151) are inadequate, and the operating range is too narrow, thus not meeting the design requirements. In addition, if the axial tandem diffuser is used, the axial size of the compressor is greatly extended, which is not an optimal solution for the aero-engine.

Using the above-developed design method, a compact conformal diffuser is designed to match the original impeller. Some key geometrical parameters of the two diffusers are given in Table 3.

It can be noticed from Table 3 that the newly designed conformal diffuser can effectively achieve a large turning angle of the flow from the radial inlet to the axial outlet with the same radial size and small inlet flow angle. Moreover, the diffuser axial length becomes smaller. Fig. 13 compares the aerodynamic performances of the previous tandem diffuser and the new diffuser. To obtain the relative values, the isentropic efficiency of the two types of diffusers is divided by the efficiency of the new conformal diffuser at the design point.

It is evident from this figure that the new conformal diffuser outperforms the axial tandem diffuser with a 20.6% increase in the total pressure ratio and a 10.2%

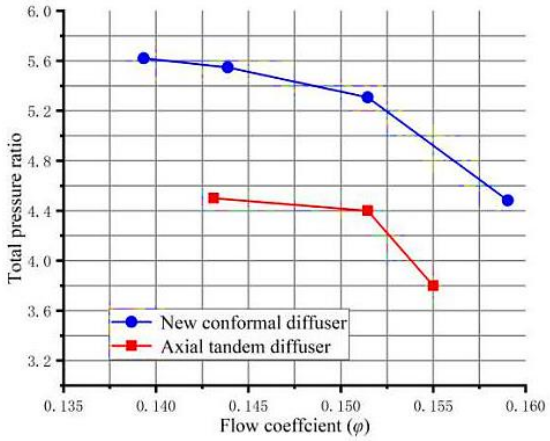

(a) Total pressure ratio

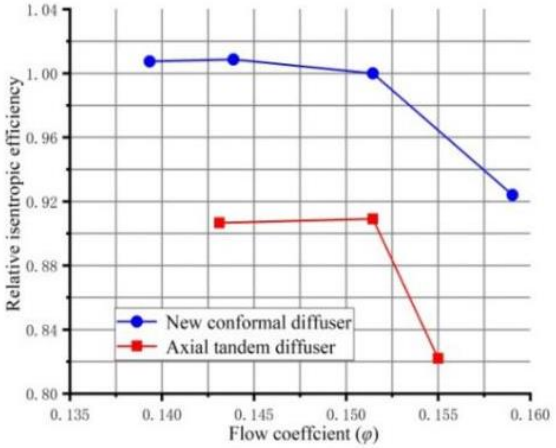

(b) Relative isentropic efficiency

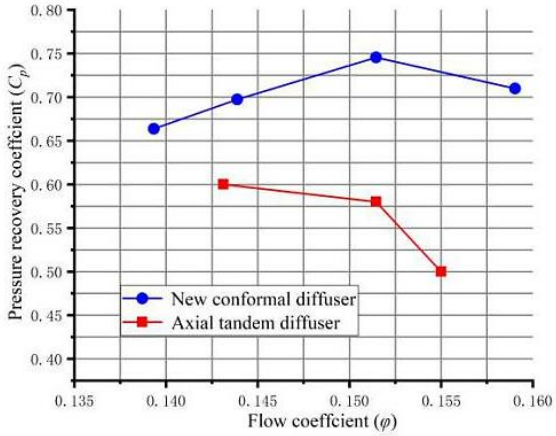

(c) Static pressure recovery coefficient

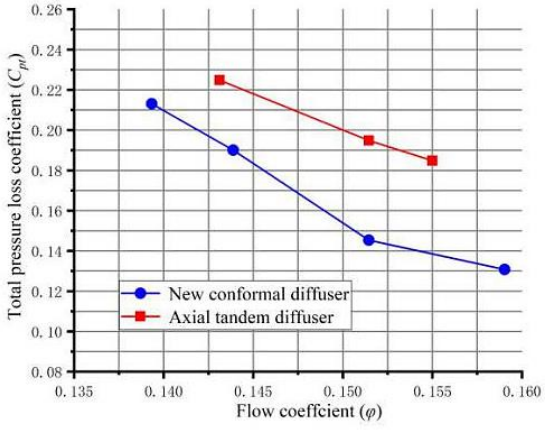

(d) Total pressure loss coefficient

Fig. 13. Performance comparisons for two diffusers of case A.

Table 3 Key parameters of the case A compressor

Parameter	Variable	Tandem	Conformal
Relative size of shroud	D_5/D_2	1.33	1.33
Relative size of hub	D_4/D_2	1.17	1.17
Relative position of diffuser inlet	D_3/D_2	-	1.02
Axial length ratio	l_{23}/l_{13}	0.48	0.31
Number of impeller blades	Z_{imp}	7+7	7+7
Number of diffuser blades	Z_{dif}	Z_{dif1}=19; Z_{dif2}=21	Z_{dif}=19
Diffuser inlet blade angle	β_{3A}	-	20°
Design speed	*rpm*	59000	59000
Total pressure ratio of impeller (at design)	ε_2	5.75	5.75
Outlet Mach number of impeller (at design)	Ma_2	1.05	1.05
Flow coefficient (at design)	φ	0.151	0.151

increase in the isentropic efficiency at the design point. Moreover, it has a wider operating range and higher C_p and C_{pt}.

The CFD results obtained for the compressor with the new conformal diffuser fully meet the design requirements for the limited radial size. However, it should be noted that there is still potential for improvement in the design of the impeller and conformal diffuser.

5.2 Case B

To further demonstrate the advantages of the new conformal diffuser, an original diffuser consisting of a radial splitter diffuser followed by an axial diffuser was replaced by a conformal diffuser for the HECC compressor. The HECC is an improved version of the NASA CC3 compressor, and its diffuser was redesigned to minimize the maximum outlet diameter, resulting in a decrease of D_5/D_2 from 1.87 to 1.45 (Medic et al. 2014). To further reduce the radial size of the HECC while maintaining similar performance to the baseline, a new conformal diffuser was designed in this study. The meridional channel comparison between the original diffuser and the new conformal diffuser is shown in Fig. 15. The main geometrical parameters of the two diffusers are given in Table 4. As shown in Table 4, the maximum outlet diameter is significantly reduced compared with the original design, and D_5/D_2 is decreased from 1.45 to 1.28.

The 3D internal flow in the axial tandem diffuser shown in Fig. 14 appears to be disordered. There is obvious flow separation near the pressure side of the second row of vanes at the inlet and the suction side near the outlet. However, the overall flow in the new

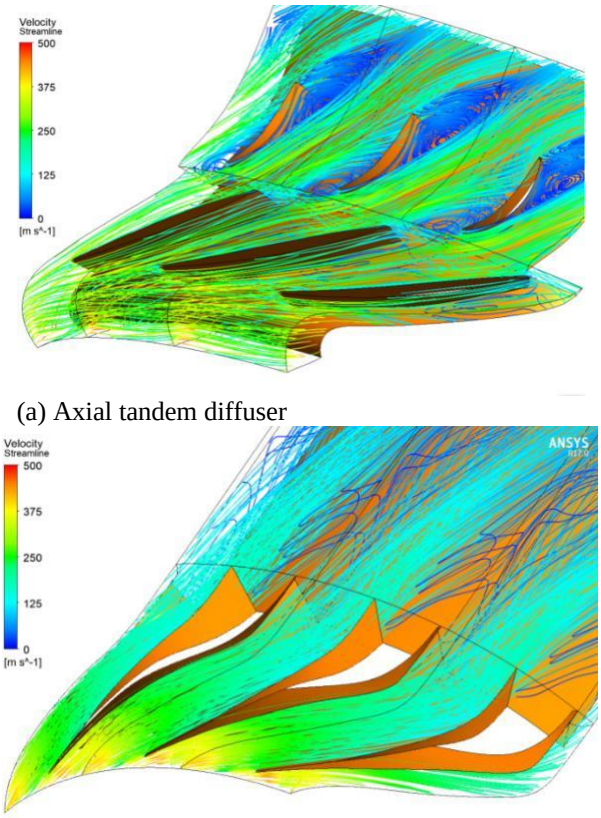

(a) Axial tandem diffuser

(b) New conformal diffuser

Fig. 14. 3D streamline comparisons for the two diffusers of case A at the design point.

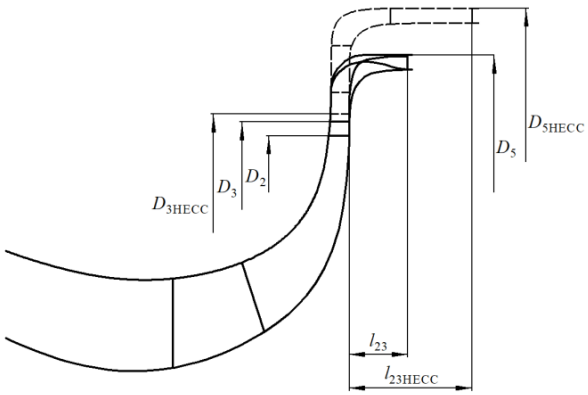

Fig. 15. Meridional channel comparisons for two diffusers of case B.

conformal diffuser is stable, and there is no obvious flow separation except for the wake flows behind the diffuser vanes.

The aerodynamic performance comparison between the original HECC and the new HECC with a conformal diffuser is shown in Fig.16. As shown in Fig. 16 (a) and (b), the performance curves for both the total pressure ratio and the isentropic efficiency for the new HECC are shifted upward compared with the original diffuser, indicating an improvement in aerodynamic performance. At the design point, the total pressure ratio and isentropic efficiency are increased by 3% and 2%, respectively. The

Table 4 Key parameters of the case B compressor

Parameter	Variable	Original	Conformal
Impeller outlet diameter [mm]	D_2	431.5	431.5
Diffuser inlet diameter [mm]	D_3	464	453
Diffuser max diameter [mm]	D_5	625	554
Axial length [mm]	l_{23}	93	43
Relative size of shroud	D_5/D_2	1.45	1.28
Number of impeller blades	Z_{imp}	15+15	15+15
Number of diffuser blades	Z_{dif}	Z_{dif1}=20+20; Z_{dif2}=60	Z_{dif}=23
Design speed	*rpm*	21789	21789
Total pressure ratio of impeller (at design)	ε_2	5	5
Outlet Mach number of impeller (at design)	Ma_2	0.98	0.98

static pressure recovery coefficient and the total pressure loss coefficient for the two different diffusers are shown in Fig. 16 (c) and (d), respectively. The improvement for the new diffuser can be observed in the figure, which is consistent with the overall compressor performance.

The 3D flow fields inside the two diffusers of the HECC at the design point are compared in Fig.17. It can be observed from this figure that there are obvious low velocity zones or flow separations at the outlet of the radial vaned diffuser and the suction sides near the axial diffuser vanes. However, the overall flow field in the new conformal diffuser is smooth and there is no obvious flow separation except for the wake flows behind the diffuser vanes. This further demonstrates that the newly designed conformal diffuser performs well as expected. This is mainly due to proper diffusion and a short path, resulting in reduced separation and friction losses. Another issue that should be mentioned is the outlet Mach number. The Mach numbers at the outlets of the original HECC and the redesigned HECC are 0.18 and 0.24 for the design condition respectively. The redesigned HECC has a slightly larger outlet Mach number, which can be reduced to the same Mach number as the original value through an extension of the axial length and further optimization of the conformal diffuser.

6. CONCLUSIONS

A novel vane-twisted conformal diffuser concept is proposed in this study to address the challenges of limited radial and axial dimensions for high-pressure ratio centrifugal compressors. The study also proposes a unique design method for the conformal diffuser and explores different cross-sectional area distributions. To verify this diffuser configuration, two compact high pressure centrifugal compressors for aero-engines are

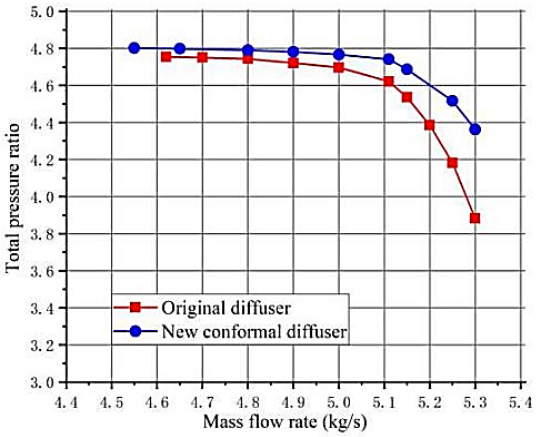

(a) Total pressure ratio

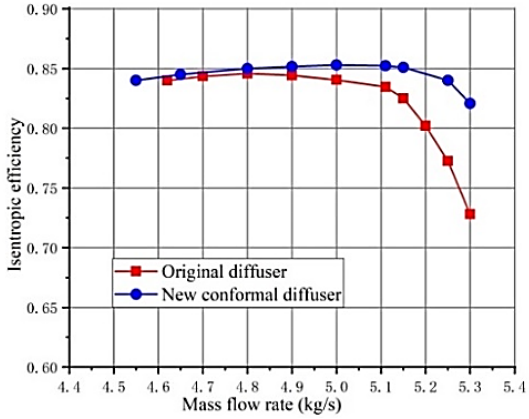

(b) Isentropic efficiency

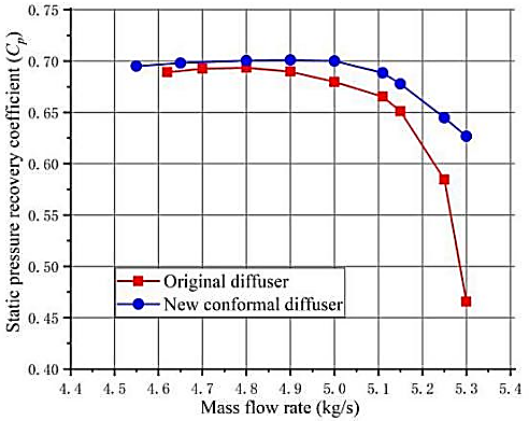

(c) Static pressure recovery coefficient

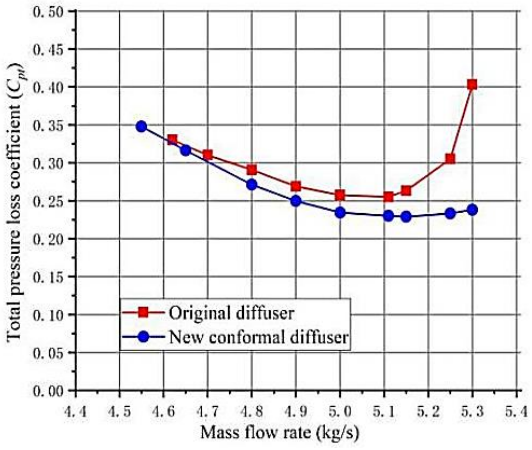

(d) Total pressure loss coefficient

Fig. 16. Performance comparisons for two diffusers of case B.

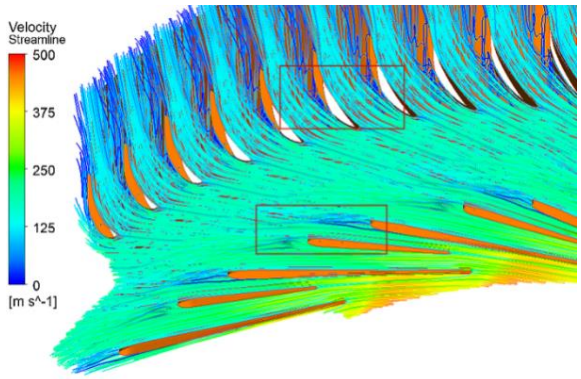

(a) Original diffuser

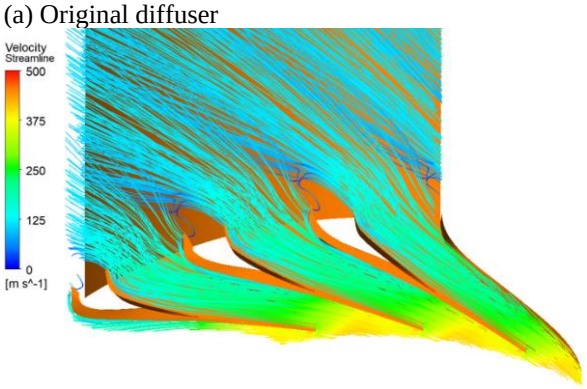

(b) New conformal diffuser

Fig. 17. 3D streamline comparisons for the two diffusers of case B at the design point.

redesigned. Numerical simulations indicate that the new conformal diffuser leads to significant improvements in the aerodynamic performance of the compressors in terms of total pressure ratio, isentropic efficiency, and operating range. In summary, the results of this study demonstrate the effectiveness of the proposed conformal diffuser design and its potential for further improvement in high pressure centrifugal compressor design. Some of the following conclusions can be drawn from the study.

1. The new conformal diffuser integrates radial, bend, and axial sections to achieve the twist design of the vane and hub. The vane and hub of the diffuser gradually convert from the turning section to form an axial section. This structure reduces the twist of the diffuser vane and changes the outlet flow of the centrifugal impeller from radial to axial through a large turning angle within a small size range. As a result, this type of diffuser can effectively reduce the radial and axial dimensions of the diffuser while ensuring the continuity of the flow channel and improving flow stability.

2. The distribution of the cross-section area is the most important factor affecting the performance of the new conformal diffuser. Three different schemes for the change of the cross-section area are compared, and it is found that there is an optimal cross-section area distribution scheme to ensure proper diffusion and reasonable static pressure recovery. The optimal distribution takes a gradual change in the section area as an example. Concave changes occur first, followed by linear changes. Adopting this optimal cross-section distribution can improve the performance of the diffuser.

3. The numerical results from the two redesigned centrifugal compressors with the new conformal diffusers demonstrate that their aerodynamic performance has improved in terms of efficiency, total pressure ratio, and operating range compared with the baseline compressors. This improvement is mainly due to the proper diffusion and shorter path, which results in smaller separation and friction losses. These results validate the effectiveness and applicability of the developed design method for the conformal diffuser. In addition, the compact design of the diffuser makes it more suitable for use in limited spaces.

ACKNOWLEDGMENTS

The authors would like to thank the National Natural Science Foundation of China (NSFC) (Grant number U1808214) and Dalian Science and Technology Innovation Fund (Grant number 2021JJ12GX010), for funding this work.

CONFLICT OF INTEREST

The authors declared no potential conflicts of interest with respect to the research, authorship, and/or publication of this article.

AUTHORS CONTRIBUTION

Xiuxin Yang: Writing original draft, Investigation, Conceptualization, Validation, Visualization, Writing - Review & Editing. Yan Liu: Validation, Resources, Supervision, Writing—Review & Editing, Funding Acquisition.

REFERENCES

Benini, E. & Toffolo, A. 2003. *Centrifugal compressor of a 100 kW microturbine: part 3—optimization of diffuser apparatus*. ASME Turbo Expo, Atlanta, Georgia, USA.

Bourgeois, J. A., Martinuzzi, R. J., Roberts, D., Savory, E., & Zhang, C. 2009. *Experimental and numerical investigation of an aero-engine centrifugal compressor.* ASME Turbo Expo, Orlando, Florida, USA.

Burger, C. J. 2016. *Design procedure of a compact crossover diffuser for micro gas turbine application.* [Doctoral thesis, the Stellenbosch University]. Stellenbosch, South Africa.

Chen, J. 2010. *Research on Transonic Micro Compressor Design Method*. [Doctoral thesis, Nanjing University of Aeronautics and Astronautics]. Nanjing, China.

Chen, J., & Huang, G. (2010) Redesign of an 11 cm-diameter micro diffuser. *Chinese Journal of aeronautics,* 23(3), 298-305. https://doi.org/10.1016/S1000-9361(09)60219-3

Chen, J., Yue, Y., & Huang, G. 2014. *Effect of vaned*

diffuser on a small centrifugal impeller performance. ASME Turbo Expo, GT2014. Düsseldorf, Germany.

Czarnecki, M., & Olsen, J. (2018) Combined methods in preliminary micro scale gas turbine diffuser design–a practical approach. *Journal of Applied Fluid Mechanics,* 11(3), 567-575. https://doi.org/10.29252/jafm.11.03.28150

De Villiers, L. C. B. 2014. *Design of a centrifugal compressor for application in micro gas turbines*. [Doctoral thesis, The Stellenbosch University]. Stellenbosch, South Africa.

Han, G., Yang, C., Li, Z., Zhao, S., & Lu, X. (2017) A review of studies on pipe diffuser of centrifugal compressor. *Acta Aeronautica et Astronautica Sinica,* 38(09)**,** 51-62. [in Chinese] https://doi.org/10.7527/S1000-6893.2017.620949

Han, G., Yang, C., Li, Z., Zhang, Y., Zhao, S., & Lu, X. (2018). High-pressure ratio centrifugal compressor with two different fishtail pipe diffuser configurations. *Proceedings of the Institution of Mechanical Engineers, Part A: Journal of Power and Energy,* 232(7)**,** 785-798. https://doi.org/10.1177/0957650917753777

Hayami, H. 2000. *Improvement of the flow range of transonic centrifugal compressors with a low-solidity cascade diffuser*. ASME Turbo Expo, GT-0465. Munich, Germany.

Jiang, J. 2016. *Research on aerodynamic design methods of a high pressure ratio centrifugal compressor*. [Master thesis, University of Chinese Academy of Sciences]. Beijing, China.

Kenny, D. P. (1969) A novel low-cost diffuser for high-performance centrifugal compressors. *Journal of Engineering for Power,* 91(1)**,** 37-46. https://doi.org/10.1115/1.3574671

Krige, D. S. 2013. *Performance evaluation of a micro gas turbine centrifugal compressor diffuser.* [Doctoral thesis, the Stellenbosch University]. Stellenbosch, South Africa.

Li, S., Liu, Y., Li, H., & Omidi, M. (2021). Numerical study of the improvement in stability and performance by use of a partial vaned diffuser for a centrifugal compressor stage. *Applied Sciences,* 11(15)**,** 6980. https://doi.org/10.3390/app11156980

Medic, G., Sharma, O. P., Jongwook, J., Hardin, L. W., McCormick, D. C., Cousins, W. T., Lurie, E. A., Shabbir, A., Holley, B. M., & Van Slooten, P. R. 2014. *High efficiency centrifugal compressor for rotorcraft applications.* Report No.: NASA/CR-2014-218114, Connecticut, USA, NASA Contractor Report; United Technologies Research Center: East Hartford.

Moustapha, H. 2003. *Small gas turbine technology: evolution and challenges.* Report No.: AAIA2559, Reston, Virginia, USA, American Institute of Aeronautics and Astronautics.

Oh, J., & Agrawal, G. L. 2007. *Numerical investigation of low solidity vaned diffuser performance in a high-pressure centrifugal compressor: Part I—Influence of vane solidity.* ASME Turbo Expo, 1009-1015. Montreal, Canada.

Oh, J., Buckley, C. W., & Agrawal, G. L. 2008. *Numerical investigation of low solidity vaned diffuser performance in a high-pressure centrifugal compressor: Part II—Influence of vane stagger.* ASME Turbo Expo, 1487-1494. Berlin, Germany.

Oh, J., Buckley, C. W., & Agrawal, G. L. X. (2012) Numerical investigation of low solidity vaned diffuser performance in a high-pressure centrifugal compressor—Part III: Tandem vanes. *Journal of Turbomachinery,* 134(6)**,** 061025. https://doi.org/10.1115/1.4006300

Roberts, D. A., LeBlanc, A. D., Kacker, S. C., Townsend, P. R. & Sasu, I. (2003). Discrete passage diffuser. U.S. Patent No. 6,589,015.

Rodgers, C. 1982. *The performance of centrifugal compressor channel diffusers*. ASME Turbo Expo, GT-10. London, England.

TCAE-CFD. *Centrifugal Compressor Benchmark HECC Stage.* https://www. cfdsupport. com/centrifugal-compressor-benchmark-hecc-stage.html

Wang, Y., Han, G., Lu, X., & Zhu, J. (2018). The influence of wedge diffuser blade number and divergence angle on the performance of a high pressure ratio centrifugal compressor. *Journal of Thermal Science,* 27(1)**,** 17-24. https://doi.org/10.1007/s11630-018-0979-2

Wrong, C. 1981. *Turbine engine design.* Report No.: AAIA0195, Long Beach, California, USA, American Institute of Aeronautics and Astronautics.

Xiang, X. U. E., Tong, W., Zhang, T., & Bo, Y. (2018). Mechanism of stall and surge in a centrifugal compressor with a variable vaned diffuser. *Chinese Journal of Aeronautics,* 31(6)**,** 1222-1231. https://doi.org/10.1016/j.cja.2018.04.003

Zachau, U., Niehuis, R., Hoenen, H., & Wisler, D. C. 2009. *Experimental investigation of the flow in the pipe diffuser of a centrifugal compressor stage under selected parameter variations*. ASME Turbo Expo, Orlando, Florida, USA.